bnhcrc.com.au

FIRE SPREAD PREDICTION ACROSS FUEL TYPES

Annual Project report 2015–2016

Khalid Moinuddin, Duncan Sutherland and Graham Thorpe
Victoria University
Bushfire and Natural Hazards CRC

Version	Release history	Date
1.0	Initial release of document	12/09/2016

Publisher:
Bushfire and Natural Hazards CRC

September 2016

Citation: Moinuddin K, Sutherland D, Thorpe G (2016) Fire spread prediction across fuel types: Annual project report 2015-2016, Bushfire and Natural Hazards CRC

Cover: The Coonabarabran bushfire threatens the Siding Springs observatory in January 2013. Photo by the NSW Rural Fire Service

TABLE OF CONTENTS

EXECUTIVE SUMMARY

Operational models that are used to predict fire behaviour can be implemented easily and rapidly. However, the operational models are only truly valid in the range of experimental conditions used to build the model. This leads to a number of difficulties when using the existing operational models to predict real-world wildfires. Physics-based modelling, that is simulating the fire behaviour from the basic equations of atmospheric fluid flow, combustion, and thermal degradation of fuel materials offers considerable insight into the dynamics of wildfire. However, physics-based simulations are computationally intensive and, at present, can only be applied to small, idealised cases. Nevertheless, the aim of this project is to use physics based models to gain insight into wildfire behaviour and use that insight to improve the current operational models for fire behaviour prediction. With this in mind, a number of investigations are underway.

The effect of a tree canopy on the near surface wind speed is investigated using Large Eddy Simulation with a view to modelling the wind reduction factor due to the canopy. The wind reduction factor is used in operational fire prediction models such as the McArthur model, to account for the reduction in wind velocity due to a tree canopy. A set of full three-dimensional simulations over idealised rectangular canopies, where the length and leaf area density of the canopy are varied, were conducted. The flow over the canopy is characterised and the potential effects on fire spread of complicated flow structures that develop at the leading and trailing edges are assessed. The simulated wind speed in the fully-developed canopy flow and the wind speed far from canopy region is used to assess the constant wind-reduction factor modelling approach.

The physics of firebrand, or ember, transport is not well understood. The distance and dispersion of the firebrands depends greatly on the turbulent fluid flow which transports the firebrands. The physics-based modelling of firebrand transport is at a preliminary stage. We seek to validate a Lagrangian particle approach for firebrand transport modelling by comparing the results from an experimental firebrand generator with simulations of same scenario. Three particle shapes, cubical, cylindrical, and disc shaped particles, representing idealised firebrands have been studied. Qualitative features of the landing distribution of the firebrands have been identified. Simulations are in progress to compare with the experimental results. So far the results are encouraging. In a related study, the thermos-kinetic properties of firebrand materials, such as bark, twigs, and leaves have been measured. This data will then be used for simulations of burning firebrands.

Fires in grasslands are prevalent in Australia, and are relatively simple to model computationally due to the uniform fuel and flat simple terrain. In the present study, the CSIRO grassland experiments are used as validation cases for the physics-based simulations. A parametric study has been conducted where the background windspeed and the grass height have been varied independently. The rate-of-spread was found to be linear with windspeed in the parameter range considered. Two simulations were conducted at different heights and correspondingly different bulk density, representing grass which had been cut and left on the ground. The fire in the taller grassland was found to have a higher

rate-of-spread. Three simulations were conducted where the bulk density was kept constant as height varied. In these simulations no systematic dependence on grass height was observed.

Direct Numerical Simulation (DNS) is a numerical technique to faithfully study fluid flows by resolving all the turbulent motions instead of resorting to modelling small scale turbulence. DNS provides great insight into the physics of flows but a limited to highly idealised and numerically tractable geometries such as channels. Nonetheless, such simulations can be used to gain insight into flows which have relevance to wildfire modelling. Three flows are studied: pressure driven flow over sinusoidal roughness, mixed convective flow (flow driven by both a temperature difference and a pressure gradient), and a buoyant line plume in a confined region.

In the future, the DNS work will contribute to improved turbulence and near-wall modelling used in the physics-based wildfire models. The results of simulations from physics-based wildfire models will in turn improve operational models. We eventually aim to produce models for the wind-reduction factor, improve knowledge of firespread in grasslands, and provide a model of firebrand transport, all of which can be used operationally.

END USER STATEMENT

Dr Simon Heemstra, *Manager Community Planning, NSW Rural Fire Service*

This project is tackling a range of problems in fire behaviour physics and modelling using a diverse range of approaches ranging from laboratory measurements to detailed numerical modelling. Some areas of the project, such as investigation of air flow near walls, address fundamental physical questions, while others have more direct practical application, such as the laboratory work characterising fire brand distributions. It is pleasing to see the project team have been developing linkages with other BNHCRC projects and seeking avenues for application of their work by other modelling teams, however it is not immediately clear how some of the basic research components of the project will have application within the lifetime of the BNHCRC.

INTRODUCTION

Empirical models of the spread of bushfires are operationally very effective. However they are inherently limited due to the fact that the data on which they are based cover a limited range of conditions, and we may get results that are unrealistic if we extrapolate beyond the ranges of the models. As Andrew Sullivan (2009) remarks, empirical models are based on observations, and not on theory. If we are to develop models that accurately predict the rate of spread of bushfires over a wide range of conditions, we must ensure that empiricism contributes to its complement, namely rationalism. For this, we turn to the laws of physics that are the unifying principles that permeate this project.

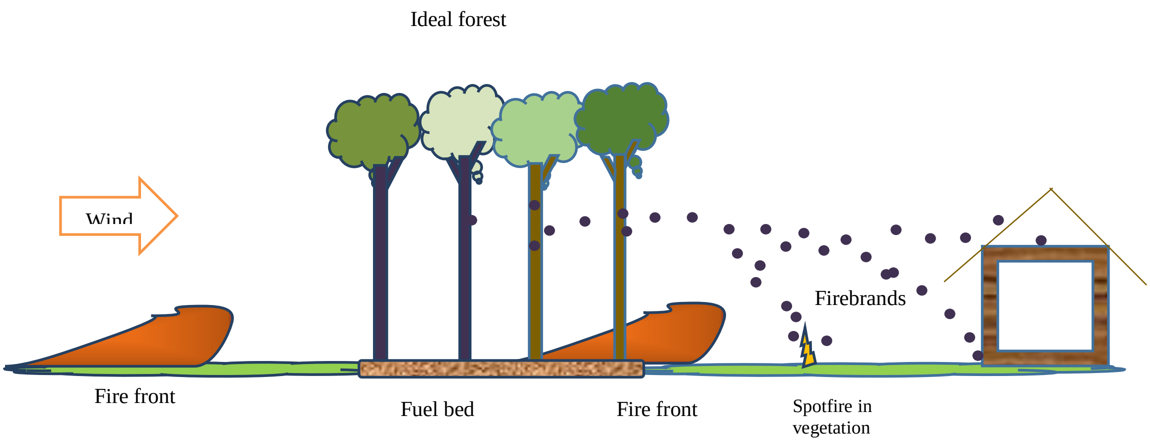

Figure 1: A schematic of fire spread mechanism in the ideal forest causing spotting in vegetation and house

The laws of physics that govern the rate of spread of bushfires appear to be immutable and universal. They also apply to all of the phenomena that we observe in bushfires. For these reasons, physics-based models are likely to underpin the next generation of bushfire models.

Figure 1 represents an ideal scenario that we are attempting to simulate in unprecedented detail and in the process obtain useful application tools for end-users. To address existing gaps in the mathematical/computational modelling of bushfire dynamics, the scenario shown in Fig. 1 is subdivided into a number of subprojects.

The rate at which fires spread is strongly dependent on the wind speed. This is true for fire over open grassland as well as through forests. The velocity profile of the wind within forests is quite different from that over open ground. The dependence of wind speed reduction on forest canopy length and density of vegetation will be explored. By comparing wind profiles entering and leaving the canopy we will develop a tool to determine an appropriate WRF. We aim to include the variation in WRF with canopy height.

The rate of spread of bushfires is often dominated by embers and firebrands being conveyed ahead of the firefront. The research group is harnessing its expertise in aerodynamics to design, construct and operate an ember generator to accurately quantify how embers disperse. This project will generate experimental data to (a) analyse the dynamics of short-range spotting and (b) develop a physics-based submodel to simulate the transport of firebrands. The latter can be further utilised to study behaviour of firebrand transport under different weather, vegetation and terrain conditions.

Grassfires can result in the loss of houses. We are conducting physics based modelling of grassfire propagation by studying the interaction of the atmosphere with grass, and quantifying the heat, mass and chemical phenomena. The current focus is on the effect of wind speed on the rate of fire spread over flat terrain and uniform distribution of vegetation. The results will be compared against the McArthur model and CSIRO model.

The evolution and dynamics of bushfires is very sensitive to the details of the rugged terrain over which they travel. These details range from leaves measured on a scale of a few centimetres, branches measured on the scale of metres to hills and mountains measured on the scale of kilometres. In a computer simulation, it would be impossible to fully simulate the exact physics on all these length scales. These elements of the terrain also obstruct wind and supply fuel, moisture and heat. Thus, a reliable boundary condition must capture the aggregate effect of the pertinent physics from all the geometrical length scales, convective heat transfer from earth surface and mass exchange through surface elements.

We are working towards a parameterisation of the near-ground flow which includes the effect of the heated earth surface, flow through the canopy (which is inherently rough), and flow above the rough canopy.

The key motivation of our work is to improve wildfire modelling so that risks and losses can be reduced. Results from all these subprojects will be utilised to develop application tools for fire behaviour analysts/regulators.

THE PROJECT - ACHIEVEMENTS

MODELLING AIR FLOW THROUGH CANOPIES

The rate-of-spread of the boundary of a wildfire depends on the wind speed. The presence of a tree canopy will act as an aerodynamic drag force and reduce the wind speed. In, for example the McArthur (1967) model, this effect is modelled by using a wind-reduction factor (WRF). The WRF is often defined as the ratio of the wind speed at 10 m height, in the open far from any canopies, to the wind speed at 2 m height within the canopy (Moon, 2016a). The sub-canopy height of 2 m is selected to represent the mid-flame height, which is believed to be the most relevant wind spread to characterise the fire spread.

Currently, to model the WRF, fire behaviour analysts use a rule-of-thumb based on the measurements of McArthur (1967). A recent and extensive field study conducted by Moon (2016a) has demonstrated that the wind reduction factor can vary over a wind range, and depends on forest type, mean wind speed in a canopy free region, and atmospheric stability. Moon (2016b) has proposed a statistical model that could be used operationally to estimate the WRF.

The sub-canopy wind velocity has received considerable attention in the fluid mechanics and meteorological literature. For example see Harman and Finnigan (2007), Shaw (1977). Effectively, these works attempt to parameterise the mean wind speed inside the canopy. Most efforts to develop a simple model of wind velocity start with the model of Inuoe 1963. For a fully developed sub-canopy wind far from any canopy edges the velocity is well modelled by a balance between the aerodynamic drag due to the canopy and the transfer of momentum in the fluid due to the turbulence.

Large Eddy Simulation (LES) is quickly becoming the preferred tool to investigate complicated atmospheric flows. Simulations of sub-canopy winds have been successfully conducted by, for example, Mueller (2014) and Cassiani et al (2008). In this study LES is used to simulate wind flow over an idealised rectangular-shaped tree canopy. In particular we seek to characterise the development of wind speed over, within, and downstream of the canopy. We then seek to appraise a simple model of the WRF based on the model of Inoue (1963).

Methodology

In LES the equations describing conservation of mass and momentum in a fluid (the continuity and Navier-Stokes equations respectively) are spatially filtered retaining the dynamically important large-scale structures of the flow. The effect of the smaller scales is then modelled.

The literature on LES for atmospheric and canopy simulations is extensive. In particular, studies by Bou-Zied (2009) show that LES can recover experimentally observed velocity profiles and higher order turbulence statistics. Therefore this simulation approach is appropriate for the present study. For a more complete discussion of LES methods see Pope (2001).

The canopy itself is modelled as an aerodynamic drag term (Mueller 2014, namely

$$F_{D,i} = \chi(x,y,z)\frac{\rho}{2}c_D\alpha(z)u_iu_i, \;.....(1)$$

where $\chi(x,y,z)$ is one if (x,y,z) is inside the rectangular canopy region and zero otherwise. The fluid density is denoted by ρ and the drag coefficient is c_D. $\alpha(z)$ is the Leaf Area Density (LAD) of the canopy, which is assumed to only vary with height. u_i is the i^{th} component of velocity (that is i represents either the x, y, or z directions.) We choose the LAD to follow a Gaussian profile following Mueller (2014). The domain considered for the first set of simulations and an outline of the LAD is sketched in Figure 2. We conduct six simulations of flow over canopies with varying LAD and canopy length between 100 and $900\,\mathrm{m}$. The LAD profiles are selected to be representative of a variety of terrestrial tree canopies Amiro (1990). The region from the ground to approximately $15\,\mathrm{m}$ represents the drag exerted by the trunks of the trees (and any intermediate forest storey). The region from $15\,\mathrm{m}$ to the top of the tree represents the leafy crown. The height of the crown $40\,\mathrm{m}$ is selected to be representative of typical forest heights throughout Australia (which are in the range of $20\,\mathrm{m}$ to $60\,\mathrm{m}$). The primary variation in the LAD of a forest is within the tree crown, the most-dense LAD considered here is representative of a dense Spruce forest (Amiro 1990), and the least dense LAD is representative of a Eucalyptus regrowth forest (Moon 2016a). The intermediate value of LAD is selected simply as a convenient value between the two extremes.

(a) Domain of simulations showing the coordinates, mean inlet profile and the canopy location within the domain. The 500 m canopy is shown.

(b) The profiles of LA) as it varies with height within the canopy. Red (triangles) most sparse canopy, green (squares) intermediate canopy, blue (circles) dense canopy.

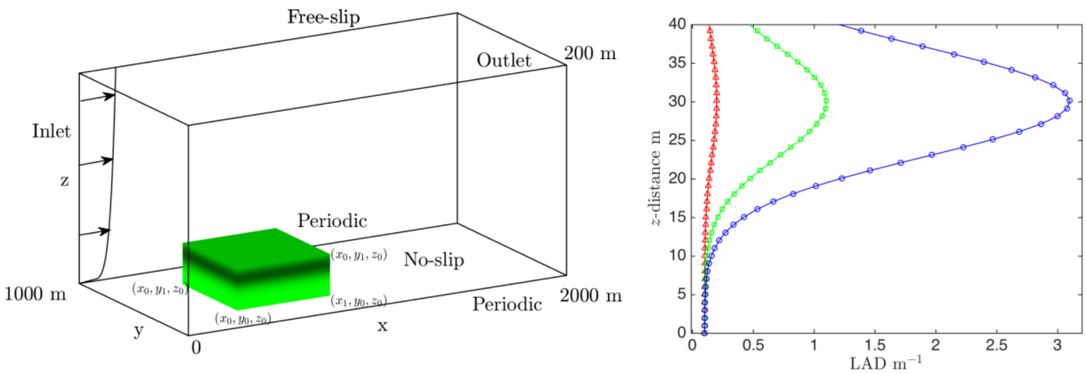

Figure 2: Simulation conditions

Results

General features of the flow: detailed examination of the a particular case

To begin characterising the flow field over the tree canopies, we firstly examine case $500\,m$ long canopy with $max(LAD) = 3.1$ in detail. The time-averaged streamlines are lines instantly tangent to the mean flow, over the canopy, within the canopy, near the edges and near the exit region of the canopy are plotted in Figure 3.

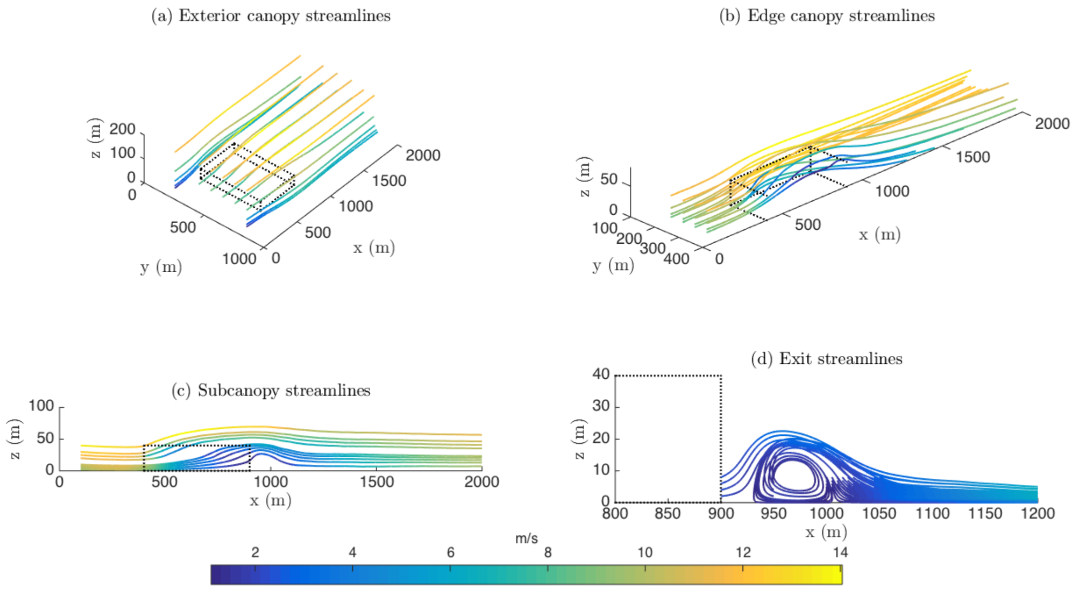

Figure 3: Streamlines within the various flow regimes. The streamlines have been constructed from the time averaged data and coloured by the velocity magnitude. (a) the streamlines around the canopy, (b) the streamlines through the canopy, (c) the edge streamlines, (d) streamlines in the recirculation region showing the presence of a large, but slowly rotating vortex.

Far upstream of the canopy, near the inlet, the imposed wind profile is a realistic ASL. Near the leading edge of the canopy an impact region is observed: the $\bar{u}$-velocity profile decreases rapidly. Correspondingly, by continuity, the spanwise, or lateral, $\bar{v}$-velocity and the vertical $\bar{w}$-velocity increase. The streamlines are pushed upwards in this region and they are also pushed towards the lateral edges of the canopy.

Near the downstream boundary of the canopy a recirculation and reattachment region may develop. A large slowly rotating vortex structure can form. This recirculation region was first investigated by Cassiani et al. (2008). Far downstream of the canopy the velocity profile starts to recover to the upstream profile.

The effect of canopy length and LAD on the centreline flow

The centreline $\bar{u}$-velocity profiles of the other canopy cases are plotted in Figure . In this case, the trunk space is sparse relative to the tree crowns, and a strong secondary maximum of velocity is seen in the impact region. This secondary maximum decays with distance along the canopy. Similar trunk space maxima have been observed by Dupont et al. (2011) and Shaw (1977). Eventually the velocity profile within the canopy will become self-similar and this is called fully developed canopy flow. For these cases, the flow does not quite fully develop before exiting the canopy. The flow above the canopy also develops and forms a wake downstream of the canopy. It is possible to use a periodic geometry, like that used by Mueller et al. (2014), to study the fully developed canopy and above canopy velocity profiles, however, the impact region and exit regions then do not exist.

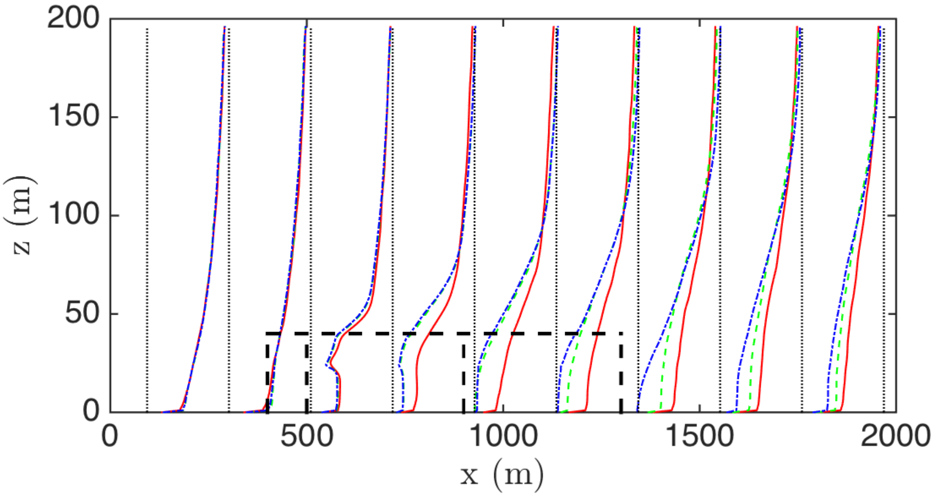

Figure 4: Centreline average streamwise velocity profiles along the 100 m (red solid), 500 m (green dashed), and 900 m (blue dotted) canopies, with fixed LAD profile. The flow develops almost identically within the canopies.

The $\bar{u}$-velocity profiles along the centreline of the domain varying with LAD are shown in Figure . Only minor differences are observable in the tree crown part of the canopy as the flow develops in the impact region. This is consistent with our modelling approach where only the leafy crown of the tree changes. Importantly, this result demonstrates that apart from near the upstream canopy edge, the leafy tree crowns to not affect the overall velocity profile. In the fully developed region, the main contribution to the drag is apparently due to the trunks and large branches. Therefore, the fully developed sub-canopy wind will not be significantly affected by the burning away of the leafy crowns.

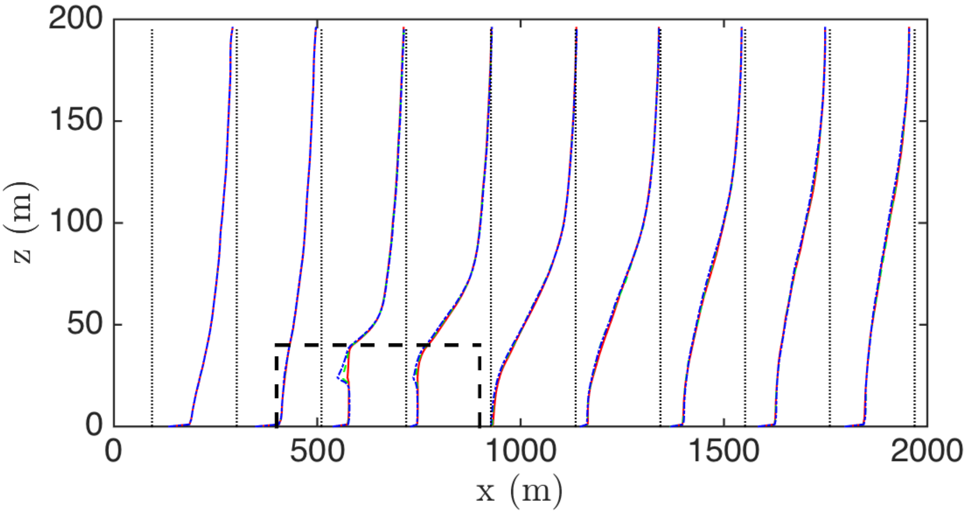

Figure 5: Variation in the average streamwise velocity profiles along 500 m canopies with variation in LAD. Red(solid): $\mathbf{max(LAD)} = \mathbf{0.2}$, green (dashed): 1.1, blue (dotted) 3.1. Note only the minor differences in the leafy crown region.

Further works

The heat generated by bushfires gives rise to buoyancy driven plumes that interacts with the wind. Because a plume entrains fluid from every direction, the recirculation region is unlikely to persist as a fire exits the canopy. However, the complicated recirculation structure may affect the transport of firebrands. The wake structures, large regions of slow moving fluid, which are shed from the canopy may impact fire behaviour for a great distance downstream. Further simulations are required to understand the effect of the canopy on the rate-of-spread, and further work is required to extend the study to a realistic, irregularly shaped, inhomogeneous tree canopy.

THE SPREAD AND DISTRIBUTION OF FIREBRANDS AND IGNITION

Firebrands generated by bushfires are the root cause of spotfires which increase the rate of spread of fire. Firebrands comprise a range of components such as species bark, twigs, and leaves. The flow of firebrands in the wind has not been studied in detail, and the existing physics-based model to describe the flow and aerodynamics of firebrand does not incorporate the effect shape and size of the firebrand. The Lagrangian particle model in which the trajectory of individual particles are tracked in the fluid flow is applicable only when the particles are small in comparison to the scale of flow. This component of the project is motivated by the need to devise comprehensive models of the dispersion of embers and firebrands, and their propensity to ignite vegetation. This is achieved by characterising key physical and chemical properties of fire brands and embers generated by a range of Australian flora, and determining their aerodynamic properties.

The design and construction of a firebrand generator

To be credible computer-generated models must be validated against experimental data. Hence a firebrand generator has been designed and constructed so that the distribution of firebrands can be modelled and measured. Previously NIST has developed a firebrand generator (Manzello et al 2010), dubbed a 'fire dragon', to study the interaction of firebrands with buildings, but the NIST generator suffers a serious deficiency. The problem is this: the outlet from which the fiery embers disgorge resembles that of a dragon's mouth set atop of a long vertical neck. As a result, the embers are conveyed around a 90° bend immediately before they are cast out horizontally. Hence, the distributions of the embers and air velocity at the dragon's mouth are highly non-uniform. We have designed a firebrand generator involving two co-axial pipes which produces uniform air velocity at the mouth as shown in Figure 6.

(a) Firebrand generator prototype (b) Air velocity distribution

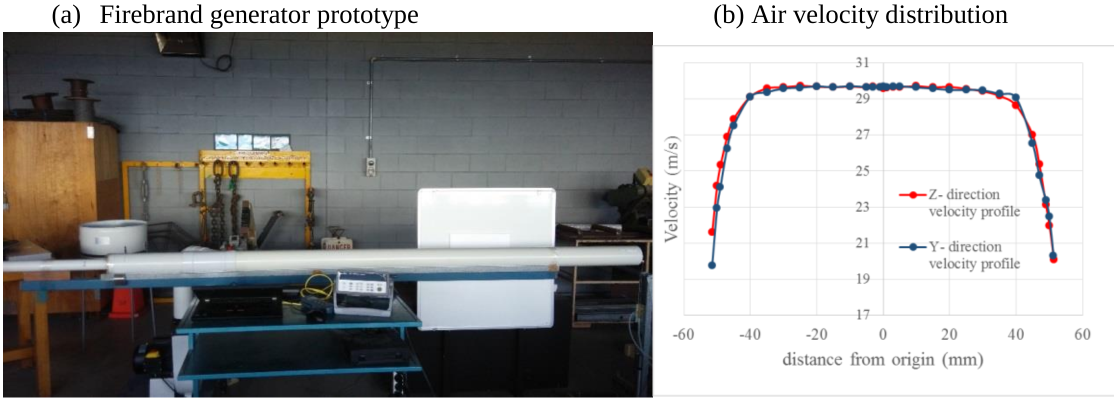

Figure 6: Firebrand generator prototype and air velocity distribution

In the present phase of the project we are comparing the experimental results with the existing computational Lagrangian particle model in Fire Dynamics

Simulator (FDS). We are also measuring the velocity of firebrands and their scattering patterns. The effect of passive firebrands shape (cubical, cylindrical and square disc shape non-burning firebrand particles) on the transport of firebrand using firebrand generator prototype is studied. The particles after falling on a firebrand collecting pad bounce and collide with each other, so to obtain accurate statistical distribution video analysis of scattering is carried out and the first impact location is measured. The average scattering plots of their first impact on the pads are shown in Figure 7. A tail is observed closer to the firebrand generator in the particle distribution shown in Figure 7 (a) and (b) for cubical and cylindrical firebrand, which is not very prominent for square disc as seen in Figure 7(c). In terms of distance traveled the order is: Cubical > Cylindrical > Square disc. We can see more spanwise scattering in the case of square disc firebrands compared to other two types. In terms of spanwise scattering the order is: Square Disc > Cylindrical > Cubical.

(a) Cubical (b) Cylindrical (c) Square Disc

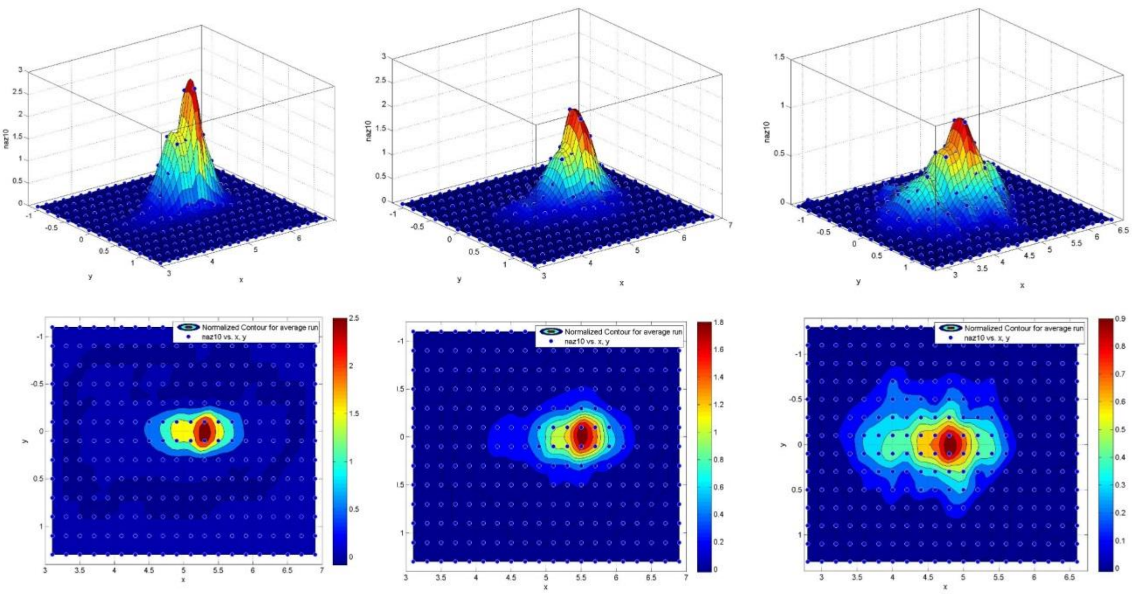

Figure 7: Normalised surface and contour plot of the first impact of firebrands

Preliminary simulations have been conducted on the transport of firebrands (cubical and cylindrical) using the physics-based model as shown in Figure 8. Qualitative agreements are observed with experimental results.

(a) Cubical (b) Cylindrical

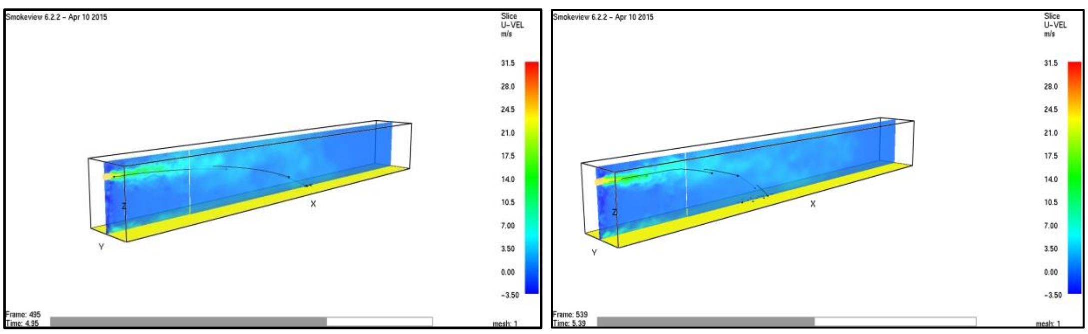

Figure 8: Simulations of firebrands dispersion

Thermo-physical, flammability and kinetics properties of fuel bed

To study the ignition of fuel bed from firebrand it is important to estimate the thermo-physical and kinetic properties of the fuel bed to improve the thermal degradation (gasification when heated prior to taking part in combustion process) sub-model of the physics-based model. The kinetic properties of forest litter are significantly different than the timber material of the same species which is observed through Fourier transform infra-red spectroscopy (FTIR) and Thermo-gravimetric analyser (TGA). Kinetic parameters of forest litter fuels i.e. bark, twigs, leaves, etc of pine and eucalyptus and grass are being estimated in the inert atmosphere of nitrogen.

Further work

A laboratory-scale firebrand generator with variable flow speed is constructed of galvanised steel which can produce both flaming and non-flaming firebrands. The equipment is ready to use for both flaming and non-flaming firebrands with minor modifications.

The kinetic parameters of forest litter fuels in oxidative environment will be measured as part of this research. Furthermore thermo-physical properties, such as thermal conductivity, thermal diffusivity, and heat capacity, and flammability parameters such as ignition time and temperature will be measured with a Hot Disc Analyser and Cone calorimeter, respectively.

EFFECT OF WIND VELOCITY AND VEGETATION HEIGHT ON GRASSFIRE PROPAGATION

This component of the project involves a systematic parametric study of a grassfire, using our physics–based model (FDS). The reference set involved an Australian grassland experiment conducted on a 100 m x 100 m plot with a nominal 4.6 m/s wind 2m above the surface. The model has four combinations of physical representation of vegetation and their thermal degradation. Of these four, the most simplistic and computationally least intensive method which combines the boundary fuel (BF) model with the linear degradation model has been employed in this study. Our numerical study shows that the model is capable of reproducing the experimental results. Following this a parametric study has been carried out by varying the wind speed and vegetation height.

Model description

The BF model treats the fuel as a thermally thick bulk fuel bed and uses a separate gas phase grid so that temperature gradients and conjugate heat transfer between the gas and solid phases in the bulk fuel bed are resolved. This grid has a sufficiently high spatial resolution to capture radiant and convective heat transfer. The assumptions leading to the BF model are most consistent with large fires for which the majority of the heat release (and, therefore, radiant emission) occurs above the fuel bed (resulting in predominantly vertical radiant heat transfer in the thermally degrading fuel bed).

The linear model assumes a two-stage endothermic thermal decomposition (water evaporation and then solid fuel pyrolysis). For water evaporation:

$$\text{If } T_s\text{=373 } K,\ \dot{m_{vap}} = \frac{\dot{Q_{net}}}{\Delta h_{vap}} \quad \text{.........(2)}$$

where, T_s is the vegetation surface temperature, $\dot{m_{vap}}$ is the evaporation rate, Q_{net} is the net energy (convection plus radiation) on the fuel surface and Δh_{vap} is the latent heat of evaporation. It uses the temperature-dependent mass loss rate expression of Morvan and Dupuy (2004) (presented as Eq 3) to model the solid fuel degradation and assumes that pyrolysis begins at 400 K.

$$\text{If } 400\ K \leq T_s \leq 500\ K,\ \dot{m_{pyr}} = \frac{\dot{Q_{net}}}{\Delta h_{pyr}} \text{ x } \frac{\dot{T_s}-400}{500-400} \quad \text{.........(3)}$$

where, $\dot{m_{pyr}}$ is the pyrolysis rate and Δh_{pyr} is the heat of pyrolysis (also known as heat of reaction). The solid fuel is represented as a series of layers that are consumed from the top down until the solid mass reaches a predetermined char fraction at which point the fuel is considered consumed. Char oxidation is not accounted for. With the linear model, ignition and sustained burning occurs more 'easily' (i.e., at lower gas phase temperatures) because pyrolysis occurs over a lower temperature range. Because of this, coarser gas phase grid resolutions may be sufficient but this requires that the user to supply a bound on the maximum mass loss rate per unit volume (kg/s/m^3).

To calculate T_s for Eq 3, Eq 4 is solved:

$$\bar{\rho}_s C_s \frac{dT_s}{\mathrm{dt}} = D\frac{\partial^2 T_s}{\partial x^2} + h\left(T - T_s\right) + \phi_{Fl\to s} \quad \text{.................(4)}$$

where, $\bar{\rho}_s$ is the vegetation bulk density, C_s is the specific heat capacity, h is the convective heat transfer coefficient , $Q_{Fl\to s}$ is the radiant heat energy on the fuel surface and D is the thermal diffusivity of the vegetation. An empirical correlation (involving surface to volume ratio, σ_s, conductivity of air, vegetation packing ratio known as leaf area index or fuel volume fraction, α_s) is used to work out h to estimate convective heating of twig/grass/stuff materials, which are modelled as a collection of cylinders. $Q_{Fl\to s}$ is calculated using a ray-tracing method from the advancing flame temperature.

Reference case and model validation

Australian grassland fires were investigated by CSIRO researchers in Australia due to the simplicity afforded by terrain and (homogeneous) fuel. Also, there is a number of experimental data available for validation. The rate of spread was considered a key factor that was studied in relation to these experiments. The Australian grassland experiment was conducted on a 104 m x 108 m plot 4.6 m/s wind was measured at 2 m above the grass surface blowing left to right. Ignition was started by two field workers at the centre of the left-hand-side. The workers then walked in opposite directions and took over 56 seconds to complete the line ignition.

In Figure 9 the fire perimeter propagation from experimental study and simulation are presented. The fire spread occurs from left to right. The fire perimeters are plotted 27 s, 53 s, 85 s, and 100 s after the start of ignition. It can be observed that fireline progression is reasonably well predicted by the physics-based model.

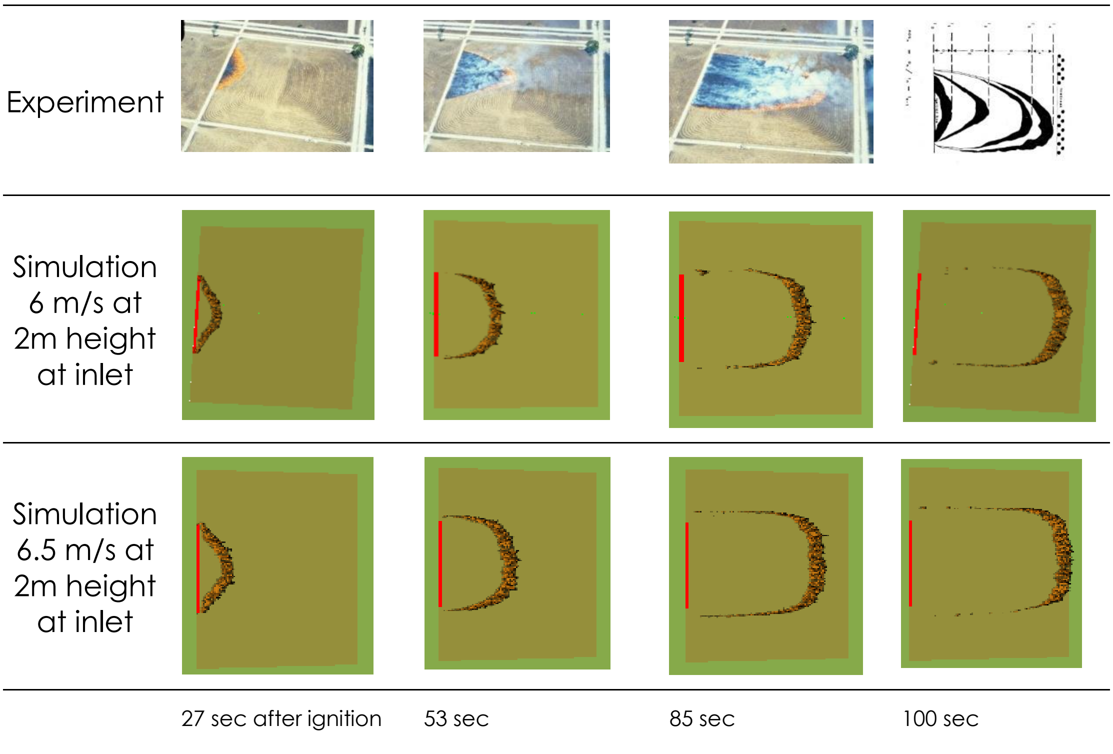

Figure 9: Model validation: fire propagation

Effect of Wind velocity

When wind speed is varied, the physics-based model has predicted faster fire spread rate than the Mk V (McArthur) model (Noble et al, 1980), but slower than the CSIRO model (Hollis et al., 2015) as shown in Figure 10. However, the numerical results predict unusually high rate of spread (ROS) when U_{10} is 3 m/s. Furthermore, the numerical result is extra-ordinarily linear (though CSIRO model is also linear beyond 6 m/s U_{10}). Both aspects need to be further analysed.

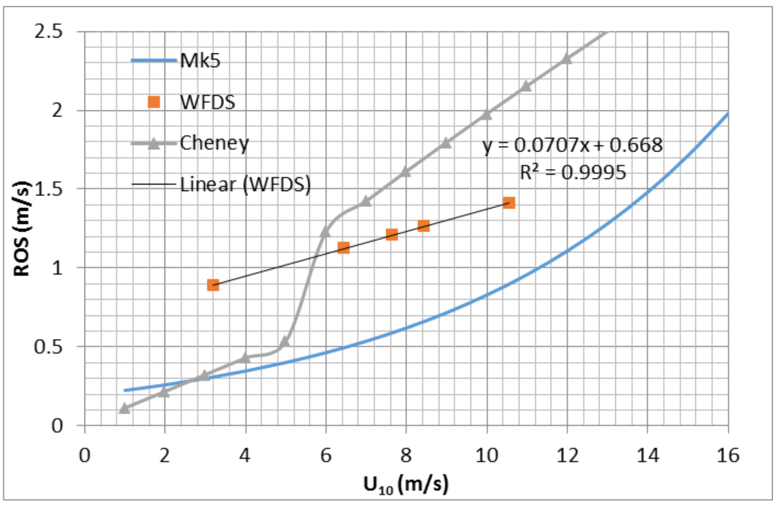

Figure 10: Effect of wind velocity on rate of spread (ROS)

Effect of grass height

Preliminary studies with simulations with two different grass heights (250mm and 160 mm) are presented in Figure 11. It should be noted that vegetation load (tonne/ha) is the same for both cases. This means in Figure 11(b) case, original 250mm high grass was mowed down to 160mm and the cut grass was still lying on the grassland. This obviously changed the bulk density ie. Case (b) had higher bulk density. The results in Figure 11 shows that fire propagated at higher rate of spread for the case (Case a), where grass height is higher and bulk density is lower. Lower bulk density promotes higher surface temperatures leading to greater pyrolysis of the grass as per Eq 3. This further leads to bigger fire (as seen in Figure 11) and quicker progression.

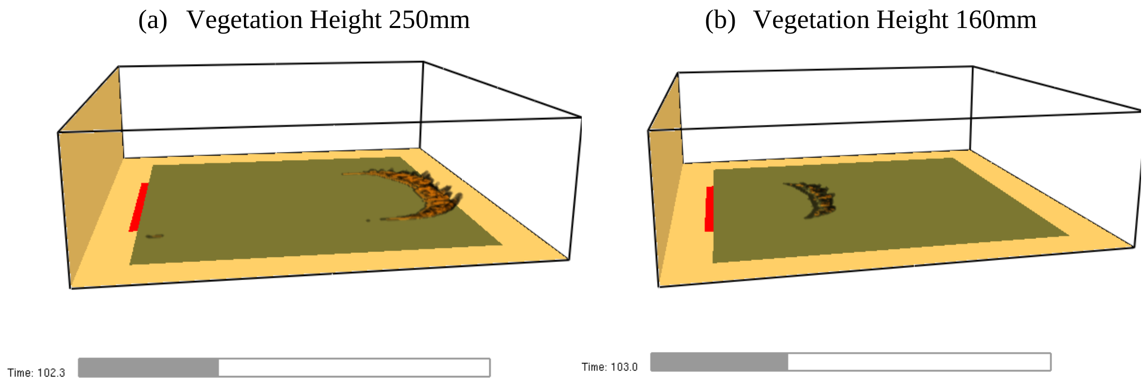

Figure 11: Effect of vegetation height

A second set of simulations was carried out three different grass heights (140, 210 and 315 mm). Here vegetation load is varied proportional to the grass height and bulk density is maintained constant i.e. no grass was considered to be mowed. The results 80 s after ignition are presented in Figure 12. No clear pattern is observed with 210mm grass, the spread is more rapid than the other two cases.

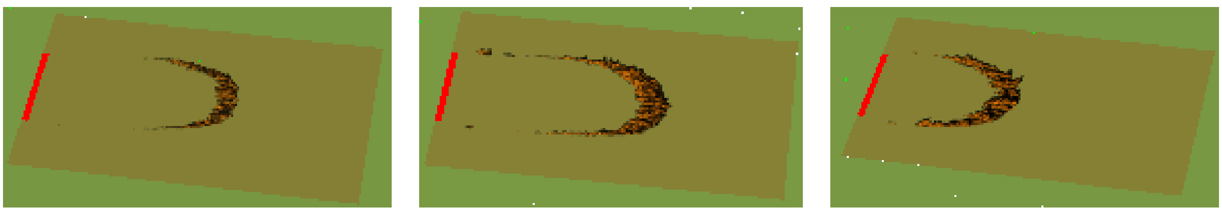

140 mm	210 mm	315 mm

Figure 12: Effect of vegetation height

AIRFLOW OVER HEATED SURFACE

When the surface of the earth is heated, the profiles of air velocity and temperature adjacent to the surface are changed. The logarithmic law of the wall is typically used to describe the mean velocity of the flow in the near wall region where the production of turbulence due to a shear flow is much larger than the production of turbulence due to buoyant effects. The law of the wall allows the shear stress to be specified as a boundary condition and allows the boundary layer velocity profile to be modelled in Large Eddy Simulations.

A well-established theory by Monin-Obukhov to predict the near surface velocity and temperature profiles over a horizontal surface exists, but it is not clear if the same theory applies to an inclined or vertical surface. The aim of this fundamental science study is to see whether an idealised law, in the boundary layer regime of the flow, much like Monin-Obukhov theory exists for a vertical surface. If the same law exists for both horizontal and vertical surfaces, it can be assumed the law would be the same for all inclined surfaces. Similarly, if different laws exist for horizontal and vertical surfaces then there will be a dependence on slope angle for inclined surfaces.

This work is of great significance to meteorology and fire prediction. Many physical scenarios involve simulating wind and temperature fields over complicated terrain. In these simulations so-called wall models are used to parameterise the near surface behaviour. Accurately representing the near-wall behaviour of the air velocity and temperature fields near non-horizontal surfaces will improve the quality of the overall simulations. Wall models that may be derived from this study could be applied to numerical weather prediction, high resolution wind modelling, and smoke transport modelling.

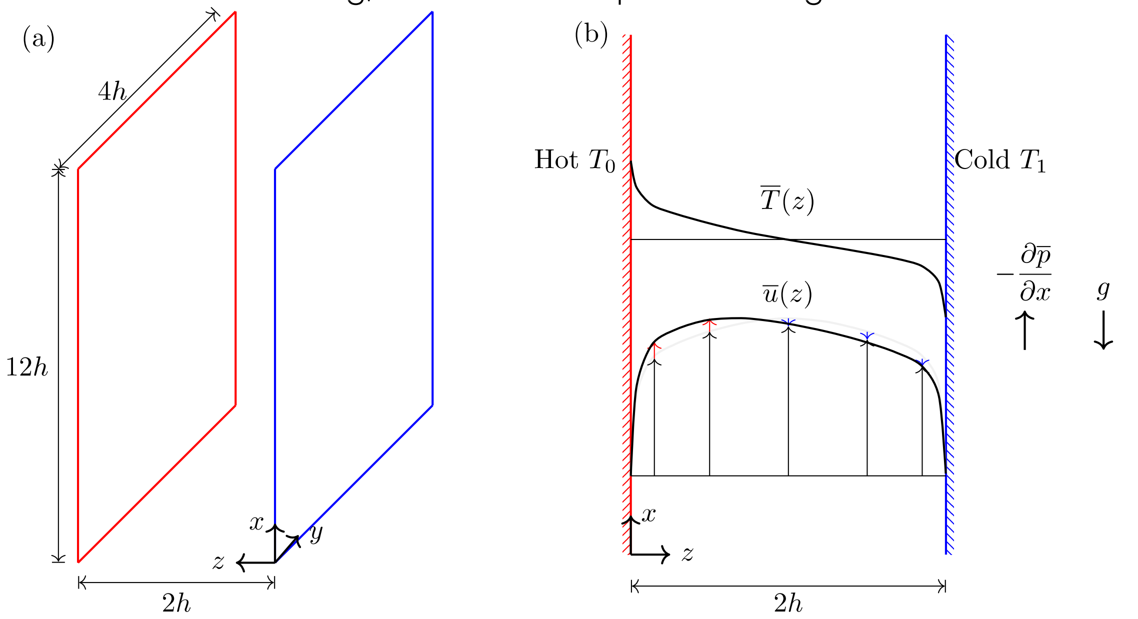

Figure 13: Sketch showing the vertical channel geometry, and the mean profiles of velocity and temperature. The effect of aiding (red arrows) flow and opposing (blue arrows) flow is also shown.

In this study, Direct Numerical Solution (DNS) of the equations that govern mixed convection flow between two differentially heated vertical plates are conducted at two Reynolds numbers (quantifying the pressure-driven flow), and seven Richardson numbers (a parameter representing the balance between buoyancy and pressure-driven flow). There are two flow regimes. One regime is called aiding flow, where buoyancy acts in the same direction as the pressure-driven flow. The second regime is called opposing flow where buoyancy acts in the opposite direction to the flow. These are analogous to an unstable, and stable atmosphere respectively. A schematic of the flow setup is shown in Figure 13.

For the low Reynolds number aiding cases, the mean velocity shows marked departure from the traditional logarithmic boundary layer profile. However, this effect is not seen in the opposing cases and both aiding and opposing cases at high Reynolds number exhibit collapse to the neutral (no buoyancy) profile. Neither the aiding nor opposing mean temperature profiles collapse well to the canonical profile for both high and low Reynolds numbers. For opposing flow cases the velocity fluctuations and Reynolds stress show significant increases from the traditional profiles. However, for aiding flow cases the opposite occurs, the velocity fluctuations and Reynolds stress decrease from the neutral profiles.

There are many examples of fluid flow over heated vertical (and inclined) surfaces, particularly in bushfire scenarios. For example, accurate predictions are required of the behaviour of fires as they interact with buildings and structures at the bushfire-urban interface.

DIRECT NUMERICAL SIMULATION OF TURBULENT FLOW OVER TRANSITIONAL ROUGHNESS

Practitioners should not have to resort of powerful computers to account for roughness in order to calculate the profile of the wind as it flows over forests and urban landscapes. This can be done by either using very complicated mathematical models, or we can seek some simple mathematical parameterisation that captures the velocity profile near the rough wall. For example, parameterisations of the near wall velocity over forests are required for numerical weather prediction. Because the flow over real-world rough surfaces would be very specific to the surface that was studied and idealised sinusoidal surface is used. Figure 14 compares a forest to the idealised surface used in this study. The following discussion is an extract from a manuscript accepted for publication in the Journal of Fluid Mechanics.

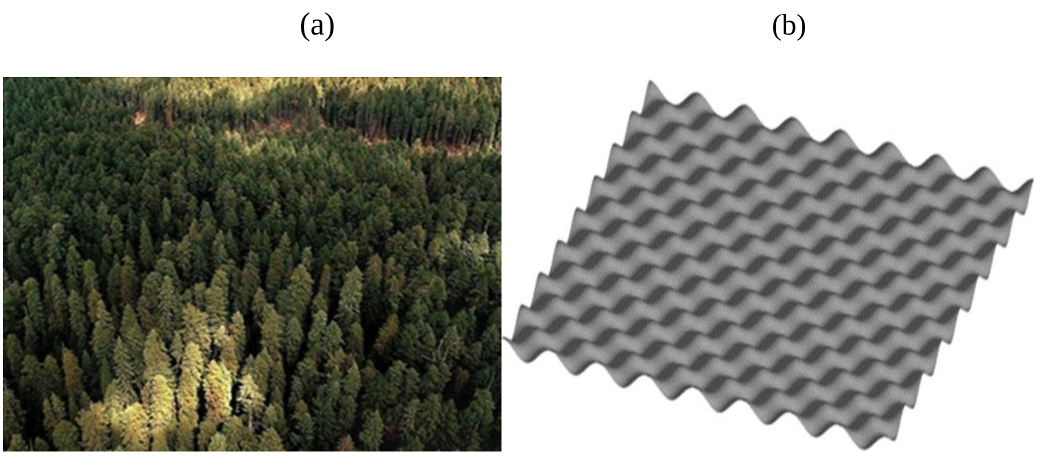

Figure 14. A forest (a) can be treated as a rough surface, but for modelling purposes that can be idealised as shown in (b). In the limit the undulations can become needle-like so that they simulate the behaviour of trees.

Roughness is characterised the solidity of the roughness. Roughly speaking solidity is the frontal area of the roughness elements which are exposed to the wind. If the solidity is low the roughness is called sparse, and if the solidity is high, the roughness is dense.

The sparse and dense regimes of roughness were investigated using direct numerical simulations of flow over three-dimensional sinusoidal roughness. The minimal-span channel technique, recently used by Chung et al. (2015) for rough-wall flows, was used. A minimal-span channel consists of a channel which is one-roughness element wide. Minimal-span channels offer considerable computational advantages over channels which are many roughness elements wide. However, minimal span channels are limited because they do not capture all of the large-scale structures that occur in the flow. The full- and minimal-span channels were seen to accurately predict the roughness function for both sparse and dense roughness. Moreover, analysis of second-order turbulence statistics showed that the root-mean-square streamwise and wall-normal velocity fluctuations were accurately captured by the minimal-span channel, especially within the roughness crest for rough-wall flows. This suggests that the large structures which are not captured by the minimal span channel are not relevant for the roughness-layer flow.

The dense regime of roughness was found to occur when the solidity was greater than approximately 0.15. In this regime, the velocity fluctuations within the roughness elements decreased, although were not negligible even for the densest case. The limit as solidity tends to infinity appears to correspond to a smooth wall in which the wall was located at the crest of the elements, and second order statistics did show the dense roughness cases were tending towards this limit. An analysis of the mean momentum balance enabled the roughness function to be decomposed into two contributions. This revealed that the primary reason for the reduction in the roughness function that is seen in the dense regime is due to the reduction in Reynolds shear stress above the roughness elements. The near-wall cycle, located at $z^+ \sim 15$ for a smooth-wall flow, is pushed up above the roughness elements, with the in the infinite solidity limit having the new near-wall cycle located at $z^+ \sim k^+ + 15$, where $k^+$is the roughness height. Spectral analysis indicates that the dense regime gradually reduces energy in the long streamwise length scales that reside close to the roughness elements. As the density increases, the long streamwise length scales are increasingly damped and the near-wall cycle is pushed up away from the wall.

DIRECT NUMERICAL SIMULATION OF A TURBULENT LINE PLUME IN A CONFINED REGION

The filling-box model of Baines and Turner (1969) of a plume in an enclosed environment is used to understand many important flows, from confined fires to building ventilation. This flow is characterised by a two-way interaction between the plume and its turbulent environment: the behaviour of the plume depends on its environment and conversely the plume modifies its environment. Despite being the basis of predictive models, the filling-box model of this two-way interaction between the plume and its turbulent environment is not well understood.

In this project, we aim to understand this flow through direct numerical simulations (DNS), which has never been attempted for this flow. DNS, which resolves all scales of turbulent motion, will enable us to examine the flow with unprecedented detail. The simulation data will then enable us to test the various assumptions that underlie the filling-box model. This project is timely in light of the recent breakthrough Finney et al. (2015) that identifies buoyant convection (as opposed to radiation) in turbulent environments as the critical (limiting) mechanism in the spread of bushfires.

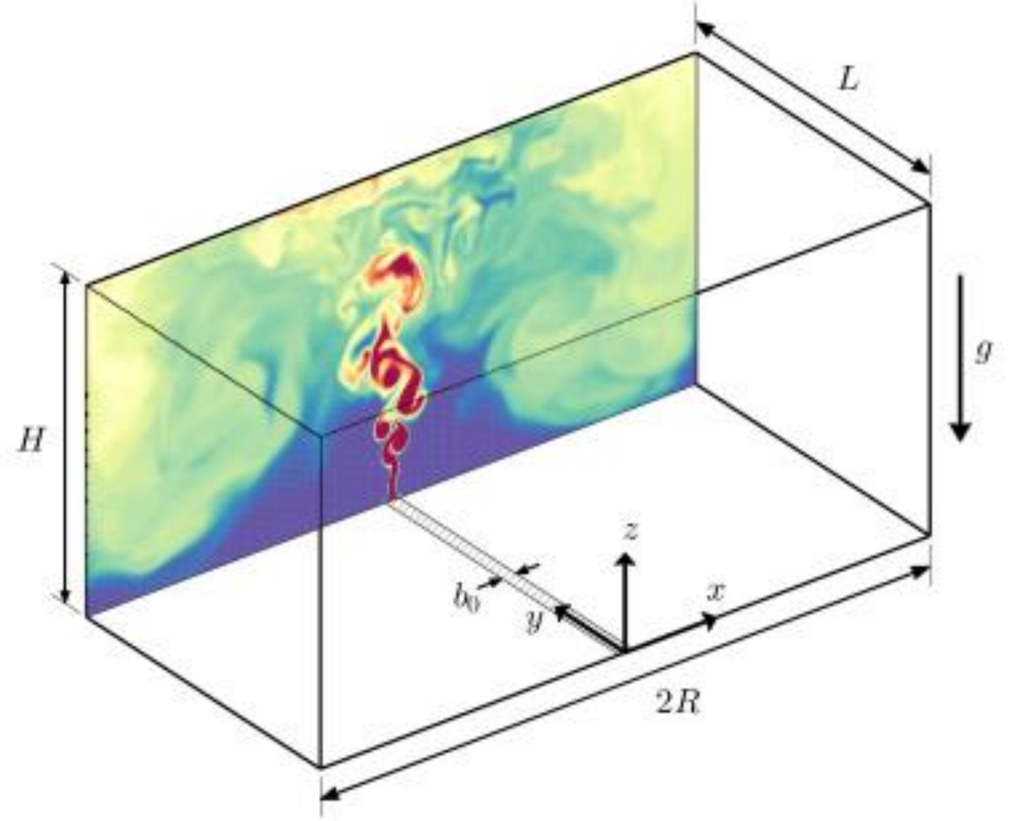

Figure 15: Schematic of a line plume in a confined region. The contours show the instantaneous temperature.

Direct Numerical Simulations (DNS) of turbulent line plumes in confined region with adiabatic side, top and bottom walls for aspect ratio, H/R = 1, where H and R are the height and half width of the box, respectively (Figure 15) have been conducted. The plume originates from a local line heat source of length, L, located at the centre of the bottom wall (z/H = 0) and it rises until it hits the top wall (z/H = 1) and spreads laterally to produce a buoyant fluid layer. Since the region is confined, the continuous supply of buoyant fluid forces this layer downwards. After this layer reaches the bottom wall, the flow is said to be the asymptotic state (Baines and Turner, 1969). In the present study, two Reynolds numbers, 3840 and 7680, are selected for plume lengths, L/H = 1, 2 and 4, where the Reynolds number of the plume is based on H and the buoyant velocity scale, $F_0^{\frac{1}{3}}$, where F_0 is buoyancy flux per unit length. The current simulations are validated against the analytical model presented by Baines and Turner (1969). The simulations exhibit a slow flapping motion of the confined line plume in the asymptotic state, which precludes a straight forward comparison with the analytical model of Baines and Turners. For the purpose of comparing with the analytical model, we have adapted a shifting method introduced by Hubner (2004). The shifted mean buoyancy profile shows improved agreement with the analytical model.

THE PROJECT - EVENTS

CONTINUING WORKING RELATIONSHIPS WITH RESEARCHERS IN FRANCE

France is subject to bushfires that are often in the vicinity in built infrastructure. This has given rise to the establishments a number of research groups that work on physics-based modelling of fires. In July 2014, Prof Graham Thorpe visited three such groups to explore the possibility of establishing links with researchers at Victoria University. The groups were located at Aix-Marseille University, the University of Lorraine, and the Institut National de la Recherche Agronomique (INRA), Ecologie des Forêts Méditerranéennes (URFM) at Avignon. An outcome of the visit was the establishment of a close working relationship with Prof Morvan at the Aix-Marseille University that has resulted in the co-supervision of a PhD student on the combustion of organic materials. Following the established relationship, Prof Morvan delivered a series of seminars to members of the project team at Victoria University in April, 2016. We also exchanged research ideas and interests and collaboration. Prof Morvan will be involved in the next phase of the project. We are currently using his FIRESTAR model for some wildfire simulations.

EFFECTIVE ENGAGEMENT

Meeting with Project Team at BoM

We had two meetings (one in 2015 and one in 2016) with Dr Jeff Kepert's Coupled Fire-atmosphere Modelling project team at BoM to exchange ideas and research findings as well as to discuss how we can compliment each other's research.

Fire behavior and Fuels Conference

Our project team members attended the Fire Behaviour and Fuels conference. There we held useful discussions with A/Prof Jason Sharples, and his students. We also met Dr Miguel Cruz of CSIRO, who is currently assisting one of our Masters students on a project titled Demystifying Bushfire Fuel Classification.

Meeting with Project Team at CSIRO

In May, 2016 we visited Dr Mahesh Prakash's DATA61 team at CSIRO to exchange ideas and research findings as well as to discuss how we can collaborate on the development of models within the SPARK toolkit.

Outcome of the engagement

There are two potential areas in which follow up projects may occur: with the CSIRO on the development of firebrand and radiation models within the SPARK toolkit, and collaboration with Jason Sharples' on sub-canopy wind modelling.

CURRENT TEAM MEMBERS

Research team

Assoc Prof Khalid Moinuddin, Victoria University
Prof Andrew Ooi, University of Melbourne
Dr Duncan Sutherland, Victoria University
Dr Daniel Chung, University of Melbourne
Prof Graham Thorpe, Victoria University
Prof Vasily Novozhilov, Victoria University

PhD students

Mr Rahul Wadhwani, Victoria University
Mr Mahfuz Sharwar, Victoria University
Mrs Jasmine Innocent, Victoria University
Mr Niteesh George, University of Melbourne
Mr Michael MacDonald, University of Melbourne

End users

Dr Simon Heemstra, Manager Community Planning, NSW Rural Fire Service
Dr Stuart Matthews, Senior Project Officer, NSW Rural Fire Service
Andrew Stark, Chief Officer, ACT Rural Fire Service
Lawrence McCoy, Senior Fire Behaviour Analyst, NSW Rural Fire Service
Chris Wyborn, Senior Technical Officer, Fire Protection Association of Australia
Mike Wouters, Senior Fire Ecologist, DENS, South Australia
Paul Fletcher, Assistant Chief Fire Officer, SAMFS
Andrew Sturgess, Fire behaviour analyst, Queensland Fire and Emergency Services
Rochelle Richards, Tasmania Fire Service

REFERENCES

1 Amiro, BD (1990). Drag coefficients and turbulence spectra within three boreal forest canopies, *Boundary-Layer Meteorology*, 52, 3, 227-246.

2 Baines, WD, Turner, JS (1969). Turbulent buoyant convection from a source in a confined region, J. Fluid Mech., 37, 51–80.

3 Bou-Zeid, E, Overney, J, Rogers, BD, Parlange, MB (2009). The effects of building representation and clustering in large-eddy simulations of flows in urban canopies, *Boundary-Layer Meteorology*, 132, 3, 415-436.

4 Cassiani, M, Katul, GG, Albertson, JD (2008). The effects of canopy leaf area index on airflow across forest edges: large-eddy simulation and analytical results, *Boundary-Layer Meteorology*, 126, 3, 433-460.

5 Chung, D, Chan, L, MacDonald, M, Hutchins, N, Ooi, A (2015) A fast direct numerical simulation method for characterising hydraulic roughness. *Journal of Fluid Mechanics*, *773*, 418-431.

6 Dupont S, Bonnefond, J-M, Irvine, MR, Lamaud, E, Brunet, Y (2011) Long-distance edge effects in a pine forest with a deep and sparse trunk space: in situ and numerical experiments, *Agricultural and Forest Meteorology*, 151, 3, 328-344.

7 Finney, MA, Cohen, JD, Forthofer, JM, McAllister, SS, Gollner, MJ, Gorham, DJ, ... English, JD (2015). Role of buoyant flame dynamics in wildfire spread. *Proceedings of the National Academy of Sciences*, *112*(32), 9833-9838.

8 Harman, IN, Finnigan, JJ (2007). A simple unified theory for flow in the canopy and roughness sublayer, *Boundary-Layer Meteorology*, 123, 2, 339-363.

9 Hollis, JJ, Gould, JS, Cruz, MG, McCaw, WL (2015) Framework for an Australian fuel classification to support bushfire management, Australian Forestry, 78:1, 1-17, DOI: 10.1080/00049158.2014.999186

10 Hubner, J, (2004) Buoyant plumes in a turbulent environment. Ph. D. Thesis, Department of Applied Mathematics and Theoretical Physics, University of Cambridge, UK.

11 Inoue, E (1963) On the turbulent structure of airflow within crop canopies. *Journal of the Meteorological Society of Japan Series 2*, 41, 317-326.

12 Manzello, SL, Hayashi, Y, Yoneki, T, Yamamoto, Y ((2010). Quantifying the vulnerabilities of ceramic tile roofing assemblies to ignition during a firebrand attack. Fire Safety Journal, Vol. 45, 35-43.

13 McArthur AG (1967) Fire behaviour in eucalypt forests. Department of National Development, Forestry and Timber Bureau Leaflet number 107. (Canberra)

14 Moon, K, Duff TJ, and Tolhurst KG (2016a) Sub-canopy forest winds: understanding wind profiles for fire behaviour simulation. *Fire Safety Journal* in press.

15 Moon, K. (2016b) Personal communication

16 Morvan and Dupuy (2004) Modeling the propagation of a wildfire through a Mediterranean shrub using a multiphase formulation *Combustion and flame* 138 (3), 199-210

17 Mueller E, Mell W, Simeoni A (2014) Large eddy simulation of forest canopy flow for wildland fire modeling, *Canadian Journal of Forestry Resources* 44, 121534–1544.

18 Noble, IR, Gill, AM, Bary, GAV (1980), McArthur's fire-danger meters expressed as equations. Australian Journal of Ecology, 5, 201–203, doi: 10.1111/j.1442-9993.1980.tb01243.x

19 Pope, SB (2001) Turbulent flows, *Cambridge University Press*, Cambridge.

20 Shaw RH (1977) Secondary wind speed maxima inside plant canopies, *Journal of Applied Meteorology*, 16, 5, 514–521.

21 Sullivan, AL (2009) Wildland surface fire spread modelling, 1990–2007. 2: Empirical and quasi-empirical models. International Journal of Wildland Fire. 2009: 18 no4: 369–386

22 McGrattan, K, Hostikka, S, Floyd, JE (2013). Fire dynamics simulator, user's guide; NIST special publication 1019.

23 Kasagi, N. Nishimura, M, *Direct Numerical Simulation of Combined Forced and Natural Turbulent Convection in a Vertical Plane Channel,* Int. J. Heat and Fluid Flow, 1997;18: 88-99.